Ukrainian Journal of Physical Optics
ISSUE 1
2024

Composite Vortex Beam Generation Using Dichroic Nematic Liquid Crystal Cell with Topological Defect

O. Krupych [1,2], T. Dudok [1], O. Mys [1], M. Kostyrko [1], I. Skab [1], Yu. Nastishin [3], T. Lavrut [3], Yu. Chahan [3], V. Nazarenko [4], O. Kurochkin [4] and R.Vlokh [1]

[1] Vlokh Institute of Physical Optics, 23 Dragomanov Str., 79005, Lviv, Ukraine
[2] Ivan Franko Lviv National University, Department of optoelectronics and information technologies, 107 Tarnavsy Str, 79012, Lviv, Ukraine
[3] Hetman Petro Sahaidachnyi National Army Academy, 32, Heroes of Maidan St., Lviv, 79026, Ukraine
[4] Institute of Physics of the National Academy of Sciences of Ukraine, 46 Nauky Aven., 03028, Kyiv, Ukraine

Received: 19.10.2023

Abstract. We demonstrate both theoretically and experimentally that a linearly polarized optical beam incident on a linearly dichroic nematic liquid crystal cell with a topological defect of the topological strength q and linear dichroism, transforms into a composite vector beam consisting of elementary vector beams with the polarization singularity orders m=2q and m=q. Consequently, it has been proved that due to the linear dichroism a liquid crystal defect of the topological strength q=1 transforms an incident circularly polarized beam into a composite vortex beam consisting of the double-charged vortex beam and vector-vortex beam with polarization order and topological charge that are equal to unity.

Keywords: composite vortex beam, composite vector beam, topological defect, dichroism, liquid crystals
UDC: 535.5
DOI: 10.3116/16091833/Ukr.J.Phys.Opt.2024.01065

1. Introduction

Optical vortices are among the intriguing objects for study in the last few decades [1]. The beams that bear optical vortices are characterized by a helical wavefront, vanishing intensity and phase uncertainty at the beam center. The azimuthal index, which is the number of phase rotations per period, is the quantized value called the topological vortex charge. Optical vortex beams find their application in novel branches of optical technologies such as microparticle manipulation [2,3], acute focusing beyond the diffraction limit [4], quantum computing [5-7] etc. Recently, a considerable attention was drawn to the composite vortex beams (CVB). The composite (also called mixed) vortex beams consist of several coaxial vortex beams of different topological charges [8]. Due to the interference, the profile the resulting beam represents quite an unusual intensity pattern built of azimuthal and radial bright and dark regions. The CVBs belong to the type of structured light beams and are more flexible in their application in comparison with single-charge optical vortex beams. A CVB can be applied for multiple particle trap [9], electromagnetically induced transparency [10], in optical communication with enhanced communication bandwidth and data transmission speed with multiplexing/demultiplexing by the orbital angular momentum [11]. One of the simplest methods of CVB generation is the method of coaxial superposition of two or more beams of different vortex charges [8]. However, in such a case, special attention should be paid to the common alignment of their waist position and parameters. The CVB can be efficiently generated using spatial light modulators [12] and metasurfaces [13].Unfortunately, the corresponding devices are quite expensive. For this reason, the method based on the hybrid binary fork gratings seems attractive [14]. However, in the last case, the optical beam changes the direction of propagation since the CVB appears in one of the diffraction maximums. Recently, we have analyzed the formation of vortices behind a dichroic nematic liquid crystal (NLC) cell with the topological defect in the director field [15]. In particular, the theoretical consideration suggests that at the half-wave phase retardation by the NLC cell and the strength of topological defect q, the emerged optical beam consists of the optical vortex beam with the charge $l=2q$ and vector-vortex beam with $l=q$, and the polarization order $m=q$ and, thus, can be considered a CVB. The present work aims to prove this prediction experimentally.

2. Method of study

To be on the same page with a reader, let us briefly recall the results recently reported by our team [15]. When an NLC cell with a topological defect of the topological strength q is illuminated by a circularly polarized plane optical wave described by the Jones vector

$$\mathbf{E}_{in}(X,Y)=E_0\begin{bmatrix}1\\ \pm i\end{bmatrix}, \tag{1}$$

where E_0 is the wave amplitude, and $\zeta(\varphi)=q\varphi$ is the angle of optical indicatrix rotation around the topological defect, φ is the tracing angle, then the Jones vector of the exiting light beam is of the form

$$\mathbf{E}_{out\mathrm{D}}(X,Y)=\sigma E_0\cos\frac{\Gamma}{2}\begin{bmatrix}1\\ \pm i\end{bmatrix}+i\sigma E_0\sin\frac{\Gamma}{2}e^{\pm i2q\varphi}\begin{bmatrix}1\\ \mp i\end{bmatrix}+(1-\sigma)E_0e^{i\{\Gamma/2\pm q\varphi\}}\begin{bmatrix}\cos q\varphi\\ \sin q\varphi\end{bmatrix}. \tag{2}$$

where $\sigma=\exp(-2\pi d\Delta k/\lambda)$ is the relative light absorption, k_1, and k_2 are the extinction coefficients of the two eigenwaves, $\Delta k=k_2-k_1$, d is the NLC cell thickness, λ is the light wavelength, $\Gamma=2\pi d\Delta n/\lambda$ is the phase difference and Δn is the optical birefringence. At $\sigma=1$ the contribution of the dichroism ($\Delta k=0$) is absent and $\sigma\to 0$ corresponds to the case when the dichroism contribution dominates ($\Delta k\to\infty$). It is seen from Eq. (2) that the first and second terms respectively describe the incident and vortex modes under the conditions of absence of dichroism. The vortex charge is $2q$. The third term is nonzero only when $\sigma\neq 1$, i.e., in the presence of linear dichroism. This term describes a vector-vortex beam with the topological charge $l=q$ and polarization order $m=q$. In the present work, we employ the polarimetric technique to check whether the CVB forms in the exiting beam. We find that for the circularly polarized incident beam, the azimuthal and ellipticity angles of the exiting beam are not sensitive to the presence of dichroism, while the situation is different for the linear polarization of the incident light.

Let the optical beam incident onto a dichroic NLC cell be linearly polarized. Due to the symmetry of the problem, the orientation of the light polarization plane can be arbitrary. For the sake of simplicity, the Jones vector of input linearly polarized light can be written as follows:

$$\mathbf{E}_{in}(X,Y)=E_0\begin{bmatrix}1\\ 0\end{bmatrix}. \tag{3}$$

Then the Jones vector of the beam exiting the cell (denoted by the subscript *out* in the sequel) is of the form

$$\mathbf{E}_{out\mathrm{D}}(X,Y) = E^{\langle 0\rangle} + E^{\langle 1\rangle} + E^{\langle 2\rangle}$$
$$= \sigma E_0 \cos\frac{\Gamma}{2}\begin{bmatrix}1\\0\end{bmatrix} + i\sigma E_0 \sin\frac{\Gamma}{2}\begin{bmatrix}\cos(2q\varphi)\\ \sin(2q\varphi)\end{bmatrix} + (1-\sigma)E_0 e^{i\Gamma/2}\cos(q\varphi)\begin{bmatrix}\cos(q\varphi)\\ \sin(q\varphi)\end{bmatrix}. \qquad (4)$$

Eq. (4) suggests that the exiting beam is a result of the superposition of three beams. Namely, the first one, $E^{\langle 0\rangle}$, corresponding to the initial linear polarization, superposes with two vector beams, $E^{\langle 1\rangle}$ and $E^{\langle 2\rangle}$. It is evident, that the term $E^{\langle 2\rangle}$ expresses the contribution of the dichroism since it approaches zero at $\sigma \to 1$ when the dichroism vanishes. Remarkably, the amplitude of the term $E^{\langle 2\rangle}$ vanishes also at $q\varphi=n\pi+\pi/2$ (*n* is an integer.

When the phase retardation of the dichroic NLC cell is $\Gamma = \pi$ (half-wave), the term $E^{\langle 0\rangle}$ is zero, and Eq. (4) simplifies to the form

$$\mathbf{E}_{out\mathrm{D}}(X,Y) = i\sigma E_0 \begin{bmatrix}\cos(2q\varphi)\\ \sin(2q\varphi)\end{bmatrix} + i(1-\sigma)E_0\cos(q\varphi)\begin{bmatrix}\cos(q\varphi)\\ \sin(q\varphi)\end{bmatrix} \qquad (5)$$

If the dichroism is absent, which corresponds to $\sigma = 1$, the term $E^{\langle 2\rangle}$ is zero, and only the term $E^{\langle 1\rangle}$ remains in Eq. (5). In such a case, only one vector beam expressed by the term $E^{\langle 1\rangle}$ forms behind the NLC cell. For the general case of a dichroic NLC cells, all three terms in Eq. 4 are nonero, thus, the reasonable question arises: how to confirm the presence of the two vector beams in the light beam exiting the studied NLC cell? To answer it using the polarimetric method, we need to calculate the 2D distribution of the polarization parameters at the exit of the dichroic NLC cell and compare the obtained maps with those acquired experimentally.

To derive the azimuth and ellipticity of the polarization ellipses behind the dichroic NLC cell we rewrite the expression for the outgoing Jones vector (Eq. 4) to the form:

$$\mathbf{E}_{out\mathrm{D}}(X,Y) = E_0\begin{bmatrix}\cos^2(q\varphi)\exp(i\Gamma/2) + \sigma\sin^2(q\varphi)\exp(-i\Gamma/2)\\ \sin(q\varphi)\cos(q\varphi)[\exp(i\Gamma/2) + \sigma\exp(-i\Gamma/2)]\end{bmatrix} \qquad (6)$$

Because of the considerable complexity of analytical expressions, further analysis implies numerical computation. The appropriate technique used for numerical calculations is based on the approach described in detail in [16]. Following this approach, first for the known Jones vector of the polarized light one calculates the so-called complex polarization variable

$$\chi = \frac{E_y}{E_x}. \qquad (7)$$

Then the azimuth ζ of the major axis and ellipticity angle ε of the polarization ellipse are

$$\varsigma = \frac{1}{2}\arctan\left[\frac{2\mathrm{Re}(\chi)}{1-|\chi|^2}\right], \qquad (8)$$

$$\varepsilon = \frac{1}{2}\arcsin\left[\frac{2\mathrm{Im}(\chi)}{1+|\chi|^2}\right]. \qquad (9)$$

We have calculated the dependences of the azimuth ζ and the absolute value of the ellipticity angle $|\varepsilon|$ as functions of the tracing angle φ for the cases with and without the dichroism for the same phase retardation value of the NLC cell with the topological defect of the strength $q = 1$ (see Fig. 1).

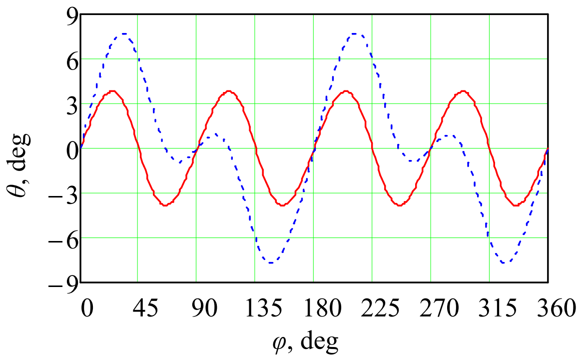

a)

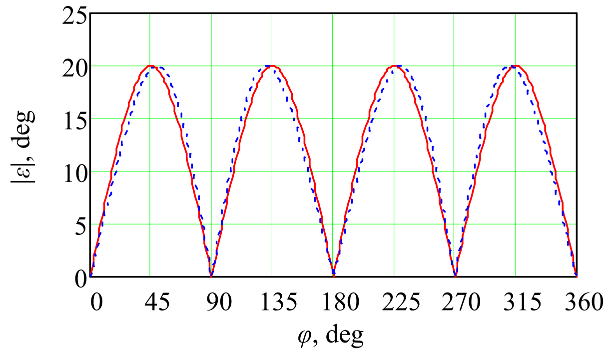

b)

Fig. 1. Computed dependences of the azimuth ζ (a) and absolute ellipticity angle $|\varepsilon|$ (b) on the tracing angle φ for the NLC cell with topological defect of the strength q = 1 and phase retardation Γ = 40 deg. Solid lines correspond to the absence of the dichroism (σ = 1), and dashed lines correspond to the the nonzero dichroism (σ = 0.85).

As seen from Fig. 1b, the maximal absolute value of the ellipticity angle $|\varepsilon|$ reaches exactly the value of the half of retardation, namely, $\Gamma/2$. This fact is very useful since it allows for the experimental acquisition of the actual retardation of the LC cell from the measured map of the absolute ellipticity angle $|\varepsilon|$. Unfortunately, the difference between the dependences of the absolute ellipticity angle $|\varepsilon|$ with and without the dichroism is relatively weak, and thus they cannot be used to detect two vector beams in the output light. In contrast, the dependences of the azimuth ζ distinct significantly for the cases with and without the dichroism, as it is well seen in Fig. 1a.

We prepared a mixture of optically transparent nematic E3100-100 (from Merck) with 0.8 wt. % of fluorescent dye Nile Red. To perform optical characterization of this dichroic nematic material, we filled it into a cell of the thickness d=20.0 μm assembled of glass substrates covered with a mechanically circularly rubbed Kapton polyimide alignment layer. The spectral dependence of the linear birefringence and dichroism has been experimentally studied by our team [17]. According to our data [17], for the used nematic Δn = 0.15 at the wavelength λ = 632.8 nm and Δn = 0.18 at λ = 532 nm. The relative absorption σ=1 at λ = 632.8 nm and σ = 0.85 at λ = 532 nm. The experimental set-up used in the present work is the imaging polarimeter described in our previous works (see e.g. [18]). The polarization of the incident light of wavelengths of λ = 632.8 nm and λ = 532 nm was linear or circular depending on the experiment.

3. 3. Results and discussion

The measured distribution of the azimuth ζ of the polarization ellipse orientation and ellipticity angle ε within the cross-section of the collimated beam exiting the NLC cell is presented in Fig. 2. A topological defect showing up as the uncertainty of the azimuthal angle ζ is clearly seen in (Fig. 2 a, c) in the center of the beam. At the circumnavigation along a closed contour with the tracing angle varying by 360 deg, the azimuth ζ of the polarization ellipse varies by 720 deg.

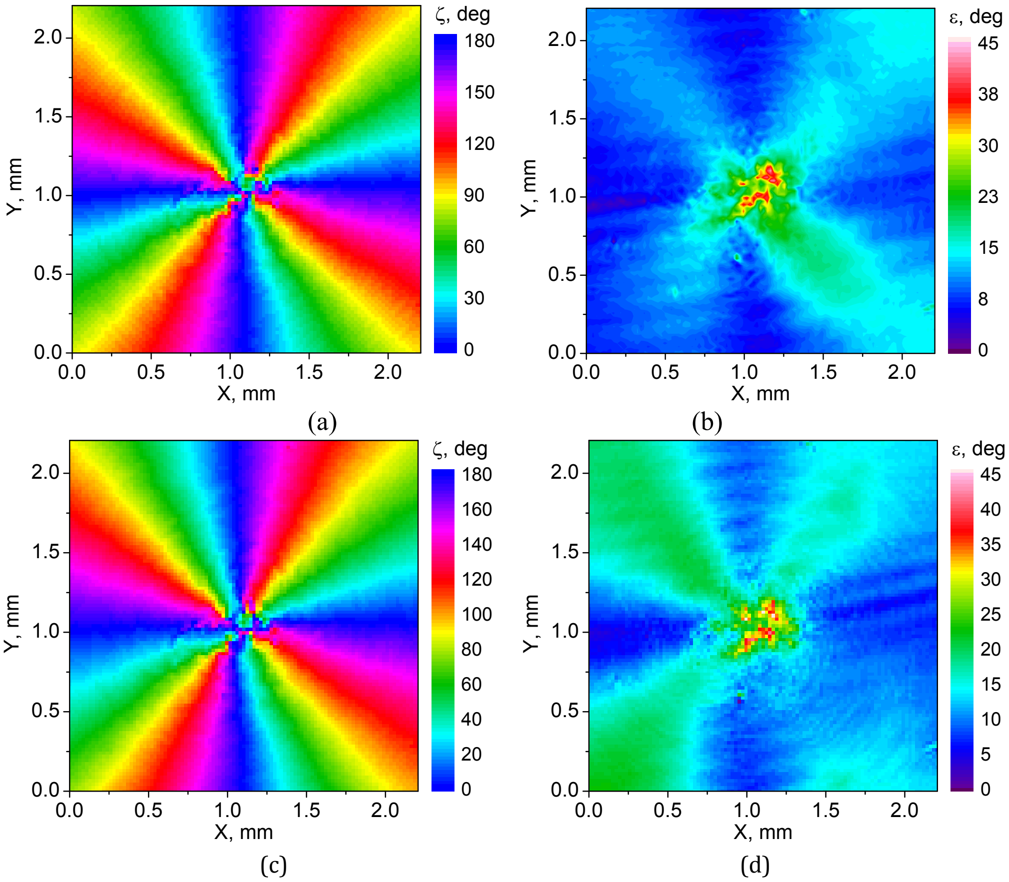

Fig. 2. Distributions of the azimuth ζ of the polarization ellipse orientation (a, c) and ellipticity angle ε (b, d) measured at λ=632.8 nm (a,b) and λ=532 nm (c,d) within the cross-section of the collimated beam exiting the NLC cell.

The distribution of the ellipticity angle ε within the cross-section of the wide beam is presented in Fig. 2 b, d. An uncertainty of the ellipticity angle is observed in the central region of the beam cross-section. Four arms of the cross expected to be observed on the maps of ellipticity angle ε are evidently distorted in the vicinity of their intersection. Observe, that at of λ=532 nm, the visibility of the arm, directed to the bottom right corner of the appears to be considerably worse in comparison with the other three arms. At λ=632.8 nm similar situation is for the arm in the left top and bottom quadrants (Fig. 2 b). The inhomogeneity in the brightness of the arms can be attributed to the inhomogeneity of the in-plane director distribution across the cell Nevertheless, the overall distribution of the ellipticity angle ε and azimuth of polarization ellipse orientation ζ suggests that we deal with the topological defect with a strength equal to unity.

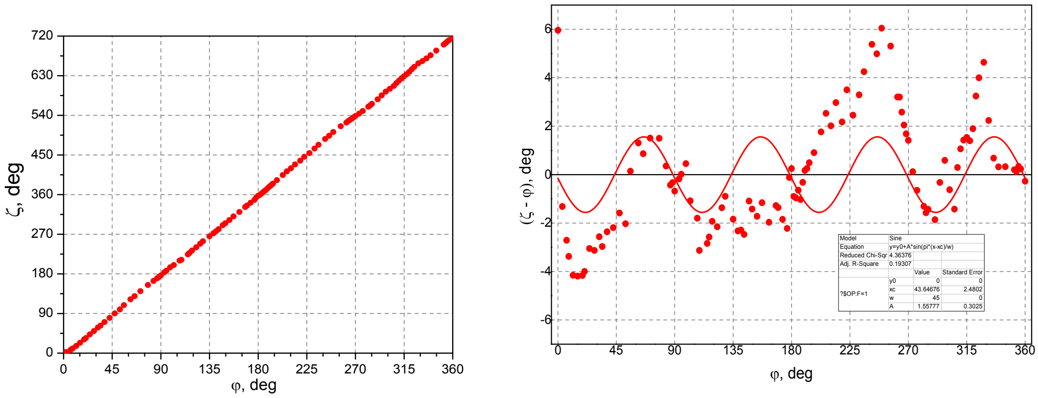

Fig. 3. Dependence of the azimuth of polarization ellipse orientation ζ on the tracing angle φ (a) and difference of the angle of the azimuth of polarization ellipse orientation ζ and the doubled tracing angle 2φ on the tracing angle φ for λ=632.8 nm. Full circles depict experimental data, solid curve – fitting by the Eqs. 6-8 (the radius of the data collection ρ = 0.73 mm).

It is seen that the dependence of the azimuth of polarization ellipse orientation ζ on the tracing angle for λ=632.8 nm (Fig. 3 a) is close to a linear dependence, though with a slight deviation. The corresponding deviations show up in the oscillations of the value ($\zeta - 2\varphi$) with the variation of the tracing angle φ (Fig. 3 b, solid curve). The amplitude of these oscillations is relatively small and does not exceed 2 deg, which is close to the accuracy limit of the used polarimetric method. Nonetheless, the tendency of the variation of the experimental data at the variation of the tracing angle is close to the theoretically calculated dependence. Besides, the range of tracing angle where the maximal deviation of the experimental and theoretical data is observed corresponds to the range where the ellipticity angle acquires irregular values due to the inhomogeneity of the LC cell.

The dependencies of the absolute ellipticity angle |ε| on the tracing angle for the wavelengths 632.8 nm and 532 nm (Fig. 4) are well-fitted by the corresponding theoretical dependence defined by Eqs. 6, 7, 9. For the studied NLC cell, the relative absorption, which characterizes the linear dichroism, is σ = 0.85 for the wavelength 532 nm and approaches the unit value for 632.8 nm. Accounting for the dichroism leads to certain asymmetry of the position of maxima of ellipticity angle (Fig. 5 a) and the sufficient inharmonicity in the dependence of the value ($\zeta - 2\varphi$) on the tracing angle φ (Fig. 5 b).

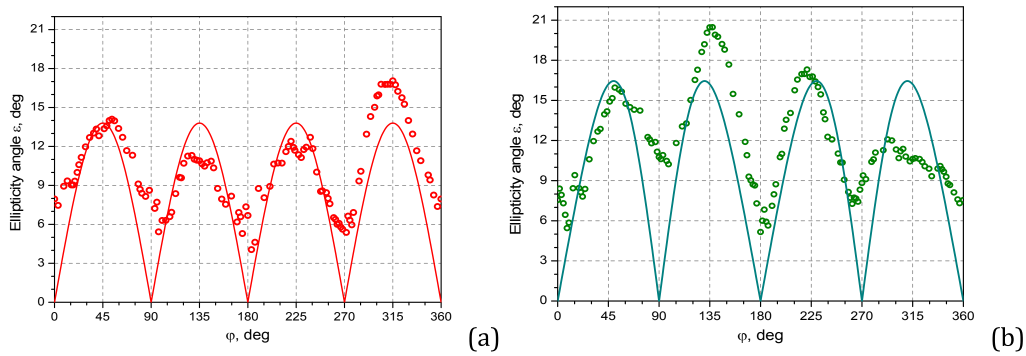

Fig. 4. Dependence of the absolute ellipticity angle |ε| on the tracing angle φ for the wavelengths 632.8 nm (a) and 532 nm (b). Open circles depict experimental data, solid curves correspond to the fitting by Eqs. 6, 7, 9 (ρ = 0.73 mm).

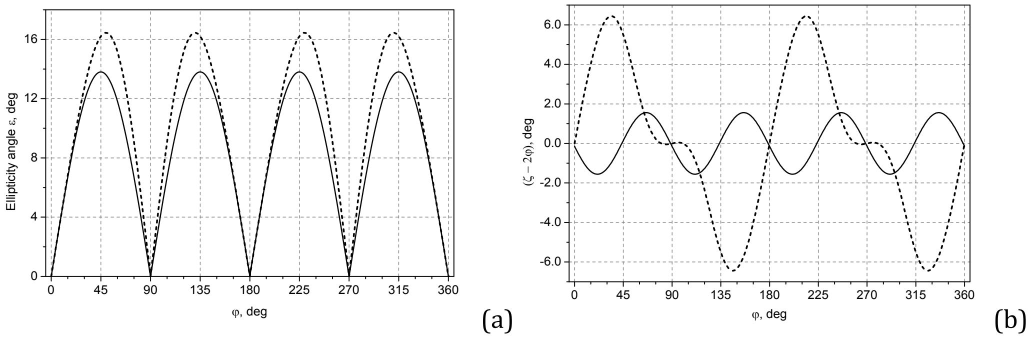

Fig. 5. Theoretical dependence of ellipticity (a) and the azimuth of polarization ellipse orientation (b) for the wavelengths 632.8 nm (solid curves) and 532 nm (dashed curves).

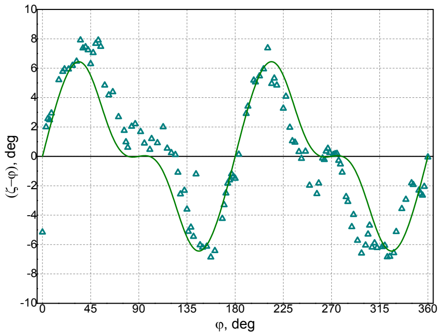

Fig. 6. Dependence of the azimuth of polarization ellipse orientation (angle $\zeta-\varphi$) on the tracing angle for λ=532 nm. Full circles correspond to the experimental data, solid curve corresponds to the fitting by the Eqs. 6–8 (ρ = 0.73 mm).

It is seen in Fig. 6 that the experimental data for the dependence of the azimuth of polarization ellipse orientation on the tracing angle well agree with those predicted theoretically when accounting for the linear dichroism. This result evidences the existence of the composite vector beam, which consists of vector beams with polarization orders m=2q and m=q. Therefore, we prove that in the case of a circularly polarized beam incident on a q=1 defect, the linear dichroism leads to the formation of a CVB consisting of the double-charged vortex beam and vector-vortex beam with the polarization order and topological charge equal to 1.

4. Conclusions

In the present work, we have theoretically shown that at the incidence of a linearly polarized optical beam on the LC cell with a topological defect with the strength q, in the case of existing dichroism, the exiting beam is a composite vector beam consisting of elementary vector beams with the polarization orders m=2q and m=q. For experimental proof of this effect, we have used the polarimetric technique, based on which one can distinguish the behavior of polarimetric parameters with and without the dichroism. In conclusion, we have experimentally shown that the presence of the dichroism leads to the formation of a composite vector beam, which consists of the vector beams with polarization orders m=2q and m=q. Consequently, we prove that the existence of the dichroism and incidence of circularly polarized beam leads to the appearance of CVB consisting of the double-charged vortex beam and the vector-vortex beam with polarization order and topological charge equal to unity for q=1.

References

1. Soskin, M.S., Vasnetsov, M.V. (2001). Singular optics. *Progress in Optics*, *42* (4), 219-276.
2. Swartzlander, G. A. Gahagan, K. T. (1996). Optical vortex trapping of particles. *Optics Letters*, *21* (11), 827–829.
3. Friese, M. E. J. Heckenberg, N. R., Rubinsztein-Dunlop, H. (1998). Optical alignment and spinning of laser-trapped microscopic particles. *Nature*, *394* (6691), 348–350.
4. Eitan Edrei and Giuliano Scarcell. (2020). Optical focusing beyond the diffraction limit via vortex-assisted transient microlenses. *ACS Photonics*, *7*(4), 914–918.
5. DiVincenzo, D. P. (1995). Quantum Computation. *Science*, *270* (5234), 255–261.
6. Kilin, S. Ya. (1999). Quantum information. *Soviet Physics Uspekhi*. *42*, 435–452
7. Boschi, D., Branca, S., De Martini, F., Hardy, L., and Popescu, S., (1998). Experimental realization of teleporting an unknown pure quantum state via dual classical and Einstein-Podolsky-Rosen channels. *Physical Review Letters. 80*, 1121.
8. Sujuan Huang, Zhuang Miao, Chao He, Fufei Pang, Yingchun Li, Tingyun Wa. (2016). Composite vortex beams by coaxial superposition of Laguerre–Gaussian beams. *Optics and Lasers in Engineering. 78*, 132–139.
9. Yuehan Tian, Lulu Wang, Gaoyan Duan, Li Yu. (2021). Multi-trap optical tweezers based on composite vortex beams. *Optics Communications. 485*, 126712.
10. Hamid R. Hamedi, Viačeslav Kudriašov, Ning Jia, Jing Qian, and Gediminas Juzeliūnas. (2021). Ferris wheel patterning of Rydberg atoms using electromagnetically induced transparency with optical vortex fields. *Optics Letters*, *46*(17), 4204-4207.
11. Jian Wang, Jeng-Yuan Yang, Irfan M. Fazal, Nisar Ahmed, Yan Yan, Hao Huang, Yongxiong Ren, Yang Yue, Samuel Dolinar, Moshe Tur and Alan E. Willner. (2012). Terabit free-space data transmission employing orbital angular momentum multiplexing. *Nature Photonics*. *6*, 488–496.
12. Mateusz Szatkowski, Jan Masajada , Ireneusz Augustyniak, Klaudia Nowacka. (2020). Generation of composite vortex beams by independent Spatial Light Modulator pixel addressing. *Optics Communications. 463*, 125341.
13. Yang Ming, Yuttana Intaravanne, Hammad Ahmed, Mitchell Kenney, Yan-qing Lu, and Xianzhong Chen. (2022). Creating composite vortex beams with a single geometric metasurface. *Advanced Materials*. *34*, 2109714.
14. Nirjhar Kumar, Ankit Arora, and Ananth Krishnan, (2021). Single-shot generation of composite optical vortex beams using hybrid binary fork gratings. *Optics Express*. *29*(21), 33703.
15. Myroslav Kostyrko, Oleh Krupych, Yuriy Vasylkiv, Ihor Skab, Rostyslav Vlokh. (2021). Topological defects related to linear dichroism. Generation of vector-vortex beams. Optik, *230*, 166335.
16. Azzam, R. M. A., Bashara, N. M. (1977). *Ellipsometry and Polarized Light*. North-Holland Publishing Company.
17. Nastishin, Yu. A., Dudok ,T., Savaryn, V., Kostyrko, M., Vasylkiv, Yu., Hrabchak, V., Ryzhov, Ye. and Vlokh R. (2021). Liquid crystal textures and optical characterization of a dye-doped nematic for generating vector beams. *Ukrainian Journal of Physical Optics*. *22*(3), 151-164.
18. Vlokh, R., Krupych, O., Kostyrko, M., Netolya, V., and Trach, I. (2001). Gradient thermooptical effect in $LiNbO_3$ crystals. *Ukrainian Journal of Physical Optics. 2*, 154–158.

O. Krupych, T. Dudok, O. Mys, M. Kostyrko, I. Skab, Yu. Nastishin, T. Lavrut, Yu. Chahan, V. Nazarenko, O. Kurochkin and R.Vlokh. 2024. Composite Vortex Beam Generation Using Dichroic Nematic Liquid Crystal Cell with Topological Defect. *Ukr. J. Phys. Opt*. 25, 01065 – 01072.
doi: 10.3116/16091833/Ukr.J.Phys.Opt.2024.01065

Анотація. *Теоретично та експериментально показано, що при падінні лінійно поляризованого оптичного пучка на рідкокристалічну комірку з топологічним дефектом з силою, рівною q та лінійним дихроїзмом, пучок, що виходить, містить композитний векторний пучок з елементарними векторними пучками з порядками поляризації m=2q і m=q. Таким чином, доведено, що при q=1 для падаючого циркулярно поляризованого пучка наявність дихроїзму приводить до появи композитного вихрового пучка, що складається з вихрового пучка з подвійним зарядом та векторно-вихрового пучка з порядком поляризації та топологічним зарядом, що дорівнюють одиниці.*

Ключові слова: *композитний вихровий пучок, композитний векторний пучок, топологічний дефект, дихроїзм, рідкі кристали*